Earth Science Informatics (2025) 18:89
https://doi.org/10.1007/s12145-024-01595-x

RESEARCH

Modelling radium equivalent activity from ^{226}Ra, ^{232}Th, and ^{40}K series of recycled waste materials: Analytical and artificial intelligence approaches

Solomon Oyebisi[1,2] · Mahaad Issa Shammas[3] · P. Jagadesh[4] · Hilary Owamah[5] · Miracle Olanrewaju Oyewola[6]

Received: 29 May 2024 / Accepted: 30 September 2024

Abstract
Primordial radionuclides in the decay sequence beginning with ^{238}U, ^{232}Th, and ^{40}K, as well as cosmic radiation, account for most of the natural radiation in environments and humans. Construction and building materials contain primordial radionuclides. This research predicts the radium equivalent activity (Ra_{eq}) from the ^{226}Ra, ^{232}Th, and ^{40}K concentrations of recycled waste materials using the deep neural networks of artificial intelligence. The Levenberg-Marquardt backpropagation technique was used to train the network, which had a three-hidden layer structure and 5–30 neurons in each layer. Predicting the Ra_{eq} of recycled waste materials was achieved with high precision using all network architectures. The best performance metrics for training, validation, and testing were demonstrated by a 3-15-15-15-1 network architecture. Furthermore, using untrained data, a robust correlation of 0.9996 R^2 was obtained from the model's confirmation.

Keywords Artificial intelligence · Recycling · Responsible consumption · Sustainability · Waste management · Waste materials

Introduction

Population growth has accelerated urbanization and industrialization, necessitating increased production of novel and inventive building materials. Various wastes are produced during the industrial and agricultural processes, and because of poor management and negligent disposal, these wastes threaten society and the environment. Recycling waste materials produced by industrial and agricultural operations for sustainable use has garnered significant interest worldwide, as it offers numerous benefits to the environment, economy, and society (United States Environmental Protection Agency 2008). The environment and human health are endangered by radiation released by certain recycled waste materials in the construction industry (Council of European Union 2014). Research on human exposure to natural radiation background levels is crucial for practical and radiological reasons, including the effects of recycled waste materials. Humans started using the materials found in their surroundings for comfort out of a need to survive. These materials may expose users to radiation, depending on the source of the raw material and the amount of radionuclide present. Radioactivity exists everywhere because of the characteristics of the climate and geology. Human activity may also raise the global radioactivity level. Research on the spread of radionuclides in the environment has provided crucial radiological data. Many studies have examined the activity concentration of naturally occurring radionuclides in recycled waste materials used as building and construction materials, giving essential details regarding the

Communicated by: Hassan Babaie.

✉ Solomon Oyebisi
sotech281.ola@gmail.com

1 Civil Engineering Department, Covenant University, Ota, Nigeria
2 Civil Engineering and Geomatics Department, Durban University of Technology, Durban, South Africa
3 Civil and Environmental Engineering Department, Dhofar University, Salalah, Sultanate of Oman
4 Civil Engineering Department, Coimbatore Institute of Technology, Coimbatore, India
5 Civil and Environmental Engineering Department, Delta State University, Abraka, Nigeria
6 Department of Mechanical Engineering, University of Alaska Fairbanks, Fairbanks, USA

radionuclide levels (Trevisi et al. 2012a; Nuccetelli et al. 2015a; Sas et al. 2017a). Naturally occurring radioactive materials (NORMs), especially those of the ^{40}K, ^{232}Th, and $^{238}U/^{226}Ra$ radionuclides, are the primary sources of radiation in building and construction materials (Council of European Union 2014). Nonetheless, prolonged ingestion, lacerations, exposure to feces, and urine containing ^{40}K, ^{232}Th, and ^{226}Ra concentrations could increase the risk of cancer (Kovler 2012; Sas et al. 2019; Puertas et al. 2021).

Modelling and predicting the radiological indexes of agricultural and industrial waste products has been investigated using artificial intelligence (AI) techniques such as artificial neural networks (ANN), deep neural networks (DNN), support vector machine (SVM), linear regression (LR), ensemble tress (ET), regression trees (RT), and Gaussian process regression (GRP) methods. These techniques have the benefit of accurately predicting complex interactions between parameters. For instance, ANN was engaged in the prediction of indoor and outdoor hazards from industrial waste products. Compared to the backpropagation training algorithms for scaled conjugate gradient (SCG) and Bayesian regularization (BR), Levenberg-Marquardt (LM) demonstrated superior performance indicators in terms of training, validating, and testing datasets (Oyebisi et al. 2023c). In contrast to RT, ET, SVM, GRP, and ANN, the LR produced the best performance metrics for forecasting excess lifetime cancer risks of agricultural byproducts (Oyebisi and Owamah 2023). The optimal performance metrics for training, validating, and testing in the internal and external hazard indexes of recycled agricultural waste materials were demonstrated by the DNN technique with a 3–10-10-10-1 architecture (Oyebisi et al. 2023a). The LR algorithm outperformed RT, ET, SVM, GRP, and ANN approaches in predicting the alpha and gamma radiation from agricultural byproducts (Oyebisi and Alomayri 2023a).

Modelling radium equivalent activity (Ra_{eq}) of recycled waste materials (RWMs) is the subject of scant research. Considering their valorization from agro-industrial wastes, RWMs are materials with natural radionuclides at varying concentrations in their composition. Therefore, products from waste materials can contribute to increasing human exposition to natural radioactivity. According to the United Nations Scientific Committee on the Effects of Atomic Radiation (UNSCEAR), various hazard-estimating models assess the radiological hazard of environmental radioactivity in a material, and one of those is the Ra_{eq} (UNSCEAR 2000). Thus, Raeq is a single index or number that describes the gamma output of various radionuclides in a material. Rather than limit every radionuclide in a material, placing a single regulatory limit on the Ra_{eq} of the radionuclides in the material becomes possible (Xinwei 2004). The justification for this investigation depends on the objectives or circumstances under which the materials are used.

This work engaged Ra_{eq} as a tool to measure the radioecological risk related to radionuclides derived from activities that yield Technologically Enhanced Naturally Occurring Radioactive Materials (TENORM) due to the recycling of waste materials, whose products contain minerals of radium and thorium, besides radioactive potassium. Datasets for the analysis were sourced from various databases. The data was trained using a 3-layer hidden DNN with 5–30 neurons. The activity concentrations (^{226}Ra, ^{232}Th, and ^{40}K) were used as input variables, while the Ra_{eq} served as the target variable. Modelling the Ra_{eq} of RWMs is a crucial aspect of the radiological framework and its safety; with the help of accurate models, possible radiological concerns can be found early in the building and construction processes, ensuring the radiological safety of RWMs.

Review and data source and collection methods used

The activity concentrations, which were limited to ^{226}Ra, ^{232}Th, and ^{40}K of RWMs, were reviewed using a thorough methodology. The review papers were based on a detailed examination of peer-reviewed works in the material sciences, building materials, and engineering domains published over the past 20 years. Data was acquired from several publishers, including Wiley, Hindawi, Taylor & Francis, Elsevier, Springer, and Multidisciplinary Digital Publishing Institute (MDPI). The references were limited to databases like Scopus, Scimago Journal & Country Rank (Sjr), and Web of Science (WoS) websites to guarantee the inclusion of only peer-reviewed references and to confirm the data collection. Additionally, it evaluated the Ra_{eq} of RWMs. In conclusion, future directions and insights were deduced. Figure 1 shows the data source flowchart.

Radium equivalent activity (Raeq)

The naturally occurring radionuclides in the materials are distributed unevenly. For this reason, the overall activities for comparing the specific radioactivity of materials containing the various radionuclides (^{226}Ra, ^{232}Th, and ^{40}K) are identified using an index called the Ra_{eq} (Shoeib and Thabayneh 2014). The gamma ray dose rate is the same for 1 Bq kg^{-1} of ^{226}Ra, 1.43 Bq kg^{-1} of ^{232}Th, or 0.077 Bq kg^{-1} of ^{40}K. In this case, the limit value of Ra_{eq} is assumed to have a yearly effect of 370 Bq kg^{-1}, comparable to the dose rate limit for public individuals of 1.0 mSv y^{-1} (UNSCEAR 2008). Managing them could avoid unnecessary exposure and possible effects on the populace. This

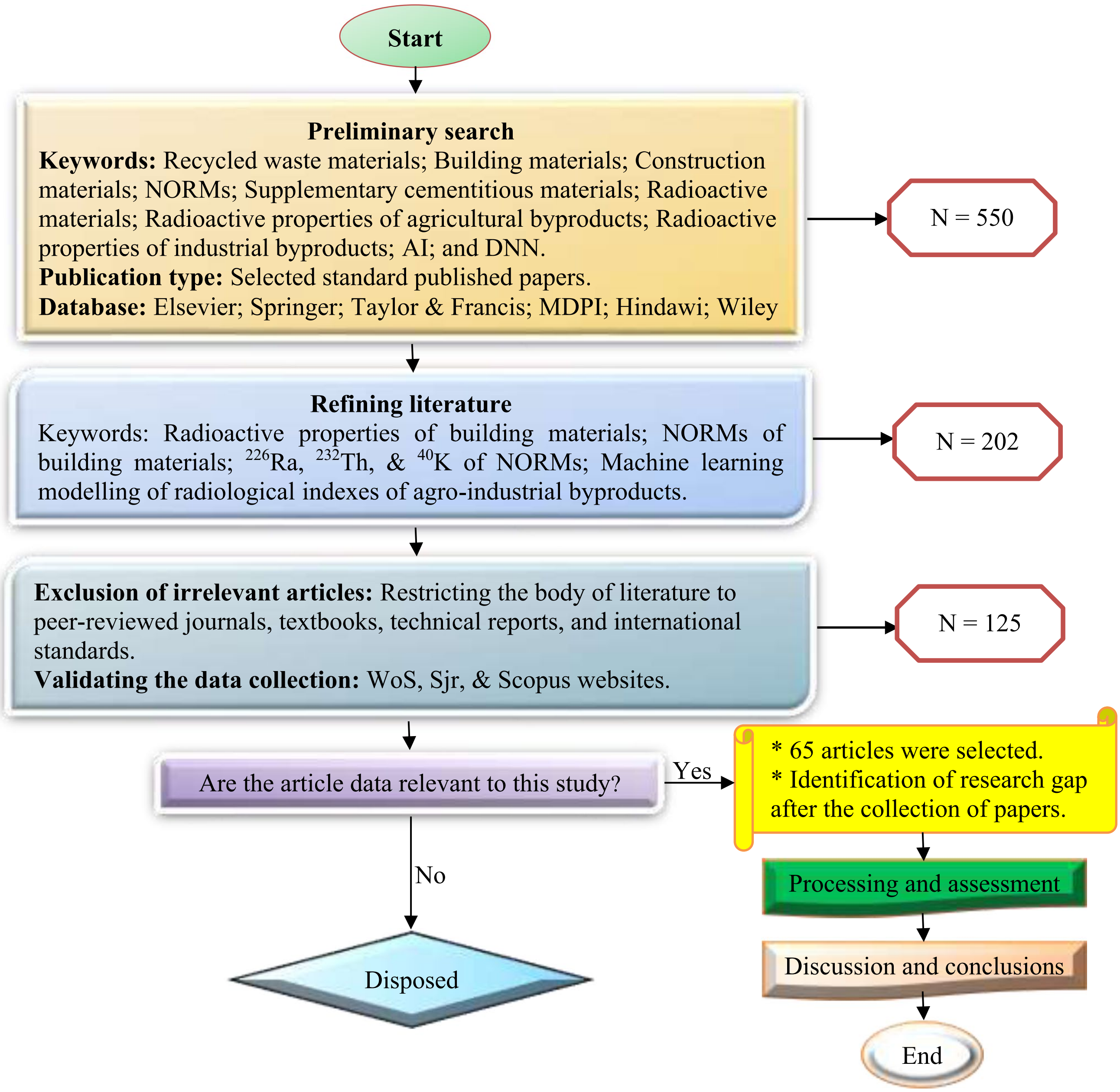

Fig. 1 Methodology flowchart

provides a different explanation for the condition of the construction materials. Therefore, Ra_{eq} is computed using Eq. (1) (Beretka and Mathew 1985; UNSCEAR 2000):

$$Ra_{eq} = \left(\frac{S_{Ra}}{370} + \frac{S_{Th}}{259} + \frac{S_K}{4810} \right) \times 370$$

where S_{Ra}, S_{Th}, and S_K represent the activity concentrations (in Bq kg^{-1}) for ^{226}Ra, ^{232}Th, and ^{40}K.

Datasets

Table 1 displays the 864 datasets that were gathered from the pertinent articles. The materials comprised recycled agricultural and industrial waste materials. The datasets were non-parametric, ignoring specific assumptions about the underlying data distribution. Ra_{eq} was also evaluated using the relations illustrated in Eq. (1).

EU MS represents European Union Member States; EC is European Commission.

Table 1 Datasets and locations

Literature						Evaluation
Material	S (Bq kg^{-1}) ^{226}Ra	^{232}Th	^{40}K	Reference	Location	Ra_{eq}(Bq kg^{-1})
Rice husk ash (RHA)	6	16	505	(Sas et al. 2019)	UK	68
mussel shell (MS)	14.1	8.5	137	(Alam et al. 2000)	Bangladesh	37
MS	9.9	6.1	96.2	(Alam et al. 2000)	Bangladesh	26
MS	12.2	5.6	110	(Alam et al. 2000)	Bangladesh	29
MS	9.8	5.7	69.8	(Alam et al. 2000)	Bangladesh	23
MS	8.8	5.3	105	(Alam et al. 2000)	Bangladesh	24
MS	8.4	4.4	81.4	(Alam et al. 2000)	Bangladesh	21
MS	0.5	1.3	198	(Krmpotić et al. 2015)	Croatia	18
MS	8.5	4.7	389	(Krmpotić et al. 2015)	Croatia	45
MS	2.0	2.3	188	(Krmpotić et al. 2015)	Croatia	20
MS	5.7	6.9	377	(Krmpotić et al. 2015)	Croatia	45
Palm oil clinker (POC)	6.89	4.46	571	(Karim et al. 2019)	Malaysia	57
POC	5.85	4.40	573	(Karim et al. 2019)	Malaysia	56
POC	6.90	4.63	571	(Karim et al. 2019)	Malaysia	57
POC	7.01	4.87	599	(Karim et al. 2019)	Malaysia	60
POC	5.56	4.21	604	(Karim et al. 2019)	Malaysia	58
POC	6.23	4.76	587	(Karim et al. 2019)	Malaysia	58
Palm oil fuel ash (POFA)	8.16	6.14	441	(Karim et al. 2019)	Malaysia	51
POFA	7.74	6.41	450	(Karim et al. 2019)	Malaysia	52
POFA	8.75	7.98	421	(Karim et al. 2019)	Malaysia	53
POFA	9.03	7.56	498	(Karim et al. 2019)	Malaysia	53
POFA	6.98	6.91	412	(Karim et al. 2019)	Malaysia	49
Bottom ash (BA)	306	65	233	(Sas et al. 2019)	UK	417
BA	113	68	623	(Sas et al. 2019)	UK	258
BA	345	59	410	(Trevisi et al. 2018)	EU MS	461
BA	423	35	296	(Petropoulos et al. 2002)	Greece	496
BA	139	108	292	(Amin et al. 2013)	Malaysia	316
BA	56	63	210	(Lu et al. 2012)	China	162
BA	62	53	457	(Mishra 2004)	India	173
BA	663	44	397	(Karangelos et al. 2004)	Greece	756
BA	114	124	210	(Yu 1996)	China	307
BA	100	105	132	(Tso and Leung 1996)	Hong Kong	260
BA	94	105	272	(Xinwei and Xiaolan 2006)	China	265
BA	70	40	355	(Puch et al. 2005)	Germany	155
BA	108	79	514	(Zeller 1995)	Germany	261
BA	541	102	714	(Schroeyers et al. 2018)	EU MS	742
BA	68	74	225	(Khan et al. 2020)	China	191
BA	70	64	457	(Fidanchevski et al. 2021a)	Macedonia	197
BA	66	97	170	(Sanjuán et al. 2019)	Spain	218
Copper slag (CS)	1135	50	585	(Schroeyers et al. 2018)	Germany	1,252
CS	770	52	650	(Schroeyers et al. 2018)	Poland	894
CS	317	54	886	(Schroeyers et al. 2018)	Germany	462
CS	317	54	887	(Zak et al. 2008)	Poland	463
CS	770	52	650	(Lehmann 1996)	Germany	894
Fly ash (FA)	119	91	438	(Sas et al. 2017)	UK	283
FA	78	126	374	(Mishra 2004)	India	287
FA	904	53	454	(Karangelos et al. 2004)	Greece	1,015
FA	100	108	388	(Alonso et al. 2020)	Spain	284
FA	88	88	868	(Alonso et al. 2018)	Spain	281

Table 1 (continued)

Literature						Evaluation
FA	188	91	343	(Schroeyers et al. 2018)	Germany	345
FA	999	200	1100	(Schroeyers et al. 2018)	Poland	1,370
FA	191	91	561	(Trevisi et al. 2018)	EU MS	364
FA	232	117	466	(Turhan 2008)	Turkey	435
FA	825	53	402	(Petropoulos et al. 2002)	Greece	932
FA	45	40	88	(Kumar et al. 1999)	India	109
FA	126	89	793	(Gökçe et al. 2020)	Turkey	314
FA	14	20	1148	(Puch et al. 2005)	Germany	131
FA	41	49	321	(Ademola and Onyema 2014)	Nigeria	136
FA	99	113	309	(Mahur et al. 2008)	India	284
FA	139	82	743	(Sas et al. 2019)	UK	313
FA	83	87	235	(Lu et al. 2012)	China	226
FA	70	79	233	(Lu et al. 2012)	China	201
FA	100	180	650	(European Commission 1999a)	EU MS	407
FA	80	207	546	(Nuccetelli et al. 2015)	EU MS	418
FA	90	66	240	(Ignjatović et al. 2017)	Serbia	203
FA	161	156	584	(Peppas et al. 2010)	Greece	429
FA	119	147	352	(Gupta et al. 2013)	India	356
FA	118	157	1463	(Khandaker et al. 2018)	Malaysia	455
FA	441	110	510	(Feng and Lu 2016)	China	638
FA	242	31	382	(Temuujin et al. 2014)	Mongolia	316
FA	263	49	216	(Temuujin et al. 2014)	Mongolia	350
FA	143	117	719	(Fidanchevski et al. 2021a)	Macedonia	366
FA	75	104	1030	(Sanjuán et al. 2019)	Spain	303
Ground granulated blast furnace slag (GGBFS)	112	52	205	(Tuo et al. 2020)	China	202
GGBFS	182	44	269	(Sas et al. 2019)	UK	266
GGBFS	179	55	172	(Sas et al. 2019)	UK	271
GGBFS	128	45	119	(Sas et al. 2019)	UK	202
GGBFS	89	140	378	(Mishra 2004)	India	318
GGBFS	151	150	14	(Alonso et al. 2020)	Spain	367
GGBFS	143	163	15	(Alonso et al. 2020)	Spain	377
GGBFS	98	89	96	(Alonso et al. 2020)	Spain	233
GGBFS	34	44	846	(Alonso et al. 2020)	Spain	162
GGBFS	32	35	632	(Alonso et al. 2020)	Spain	131
GGBFS	97	89	96	(Alonso et al. 2018)	Spain	232
GGBFS	251	25	362	(Schroeyers et al. 2018)	Germany	315
GGBFS	323	40	158	(Schroeyers et al. 2018)	Poland	392
GGBFS	100	100	500	(Schroeyers et al. 2018)	Germany	282
GGBFS	166	48	232	(Trevisi et al. 2018)	EU MS	253
GGBFS	184	135	283	(Trevisi et al. 2018)	EU MS	399
GGBFS	15	1	20	(Trevisi et al. 2018)	EU MS	18
GGBFS	336	152	786	(Trevisi et al. 2018)	EU MS	614
GGBFS	43	43	76	(Puertas et al. 2015)	Spain	110
GGBFS	178	148	243	(Turhan 2008)	Turkey	408
GGBFS	67	78	145	(Kumar et al. 1999)	India	190
GGBFS	150	65	142	(Puch et al. 2005)	Germany	254
GGBFS	35	30	75	(Puertas et al. 2021)	EU MS	84
GGBFS	160	100	250	(Puertas et al. 2021)	EU MS	322
GGBFS	270	70	240	(EC 1999a)	EU MS	389
GGBFS	251	25	214	(Sofilić et al. 2010)	Croatia	303

Table 1 (continued)

Literature						Evaluation
GGBFS	117	78	176	(Mustonen 1984)	Finnish	242
GGBFS	115	36	229	(Gallyas and Török 1984)	Budapest	184
GGBFS	115	35	192	(Zak et al. 2008)	Poland	180
GGBFS	166	48	232	(Chinchón-Payá et al. 2011)	Spain	253
Granite waste powder (GWP)	10	10	299	(Harb et al. 2008)	Eygpt	47
GWP	19	18	956	(Harb et al. 2008)	Eygpt	118
GWP	55	41	398	(El Arabi et al. 2007)	Eygpt	144
GWP	378	154	2285	(El Arabi et al. 2007)	Eygpt	774
GWP	61	48	349	(El Arabi et al. 2007)	Eygpt	157
GWP	71	96	368	(El Arabi et al. 2007)	Eygpt	237
GWP	9	1	2	(Kobeissi et al. 2013)	Lebanon	11
GWP	494	157	1776	(Kobeissi et al. 2013)	Lebanon	855
GWP	4	15	24	(Pavlidou et al. 2006)	Greece	27
GWP	91	70	1302	(Pavlidou et al. 2006)	Greece	291
GWP	2	1	49	(Krstić et al. 2007)	USA	7
GWP	170	354	1592	(Krstić et al. 2007)	USA	799
GWP	34	46	944	(Hassan et al. 2010)	Japan	172
GWP	31	45	856	(Hassan et al. 2010)	Japan	161
GWP	10	29	911	(Hassan et al. 2010)	Japan	122
GWP	12	37	742	(Hassan et al. 2010)	Japan	122
GWP	18	64	990	(Hassan et al. 2010)	Japan	186
Incinerated sewage sludge ash (ISSA)	65	60	563	(Sas et al. 2019)	UK	194
Lead slag (LS)	270	36	200	(Schroeyers et al. 2018)	EU MS	337
Metakaolin (MK)	31	34	188	(Alonso et al. 2020)	Spain	94
MK	73	63	136	(Turhan 2008)	Turkey	174
MK	125	92	695	(Turhan 2008)	Turkey	310
MK	61	44	590	(Todorović et al. 2017)	Serbia	169
MK	319	272	1470	(Todorović et al. 2017)	Serbia	821
MK	18	48	31	(Adagunodo et al. 2018)	Nigeria	89
MK	65	99	157	(Adagunodo et al. 2018)	Nigeria	219
MK	82	98	464	(Turhan 2009)	Turkey	258
Marble powder (MP)	2	1	10	(Turhan 2008)	Turkey	4
MP	1	3	25	(Petropoulos et al. 2002)	Greece	7
MP	1	4	20	(Righi and Bruzzi 2006)	Greece	8
MP	1	1	4	(Solak et al. 2014)	Greece	3
Mill tailings (MT)	87	20	226	(Kamunda et al. 2016)	South Africa	133
MT	650	90	740	(Kocsis et al. 2021)	Hungary	836
Nickel slag (NS)	52	78	76	(Schroeyers et al. 2018)	Germany	169
NS	235	45	605	(Schroeyers et al. 2018)	Poland	349
Pyrite ash (PA)	3	1	16	(Turhan 2008)	Turkey	6
PA	23	16	58	(Turhan 2008)	Turkey	50
Phosphogypsum (PG)	491	31	68	(Gezer et al. 2012)	Turkey	541
PG	629	15	10	(Turhan 2008)	Turkey	651
PG	246	50	340	(Msila et al. 2016)	South Africa	344
PG	234	21	108	(Gezer et al. 2012)	Turkey	272
PG	410	182	34	(Santos et al. 2006)	Brazil	673
PG	209	17	3	(Trevisi et al. 2012)	EU MS	234
PG	115	31	95	(Trevisi et al. 2012)	EU MS	167
PG	322	18	116	(Gezer et al. 2012)	Turkey	357
PG	306	23	17	(Trevisi et al. 2012)	EU MS	340

Table 1 (continued)

Literature						Evaluation
PG	305	20	110	(Trevisi et al. 2012)	EU MS	342
PG	440	12	235	(Trevisi et al. 2012)	EU MS	475
PG	233	30	323	(Msila et al. 2016)	South Africa	301
PG	747	14	63	(Gezer et al. 2012)	Turkey	772
PG	378	4	40	(Gezer et al. 2012)	Turkey	387
PG	618	9	24	(Gezer et al. 2012)	Turkey	633
PG	340	4	200	(Okeji et al. 2012)	Nigeria	361
PG	35	72	585	(Msila et al. 2016)	South Africa	183
PG	750	1	14	(Roper et al. 2013)	Nashville	753
Pumice (PM)	12	12	300	(Turhan 2008)	Turkey	52
PM	24	21	653	(Turhan 2008)	Turkey	104
PM	75	74	1073	(Trevisi et al. 2018)	EU MS	263
PM	462	57	1	(Trevisi et al. 2018)	EU MS	544
Red mud (RM)	310	1350	350	(Nuccetelli et al. 2015)	EU MS	7.90
RM	139	350	45	(Schroeyers et al. 2018)	EU MS	2.23
RM	380	507	361	(Nuccetelli et al. 2015)	EU MS	3.92
RM	306	408	33	(Xhixha et al. 2013)	EU MS	3.07
RM	289	285	121	(Nuccetelli et al. 2015)	EU MS	2.43
RM	97	118	15	(Schroeyers et al. 2018)	EU MS	0.92
RM	710	339	300	(Schroeyers et al. 2018)	EU MS	4.16
RM	210	539	112	(Schroeyers et al. 2018)	EU MS	3.43
RM	165	328	53	(Nuccetelli et al. 2015)	EU MS	2.21
RM	347	283	48	(Nuccetelli et al. 2015)	EU MS	2.59
RM	370	328	265	(Nuccetelli et al. 2015)	EU MS	2.96
RM	232	344	45	(Nuccetelli et al. 2015)	EU MS	2.51
RM	379	472	21	(Nuccetelli et al. 2015)	EU MS	3.63
RM	370	437	505	(Nuccetelli et al. 2015)	EU MS	3.59
RM	350	414	583	(Nuccetelli et al. 2015)	EU MS	3.43
RM	478	555	401	(Nuccetelli et al. 2015)	EU MS	4.50
RM	255	422	164	(Nuccetelli et al. 2015)	EU MS	3.01
RM	477	705	153	(Nuccetelli et al. 2015)	EU MS	5.17
RM	326	1129	30	(Nuccetelli et al. 2015)	EU MS	6.74
RM	318	1320	190	(Nuccetelli et al. 2015)	EU MS	7.72
RM	17	63	625	(Tuo et al. 2020)	China	0.58
RM	100	113	55	(Alonso et al. 2020)	Spain	0.92
RM	97	118	50	(Trevisi et al. 2018)	EU MS	0.93
RM	301	539	215	(Trevisi et al. 2018)	EU MS	3.77
RM	170	404	26	(Puertas et al. 2021)	EU MS	2.60
RM	203	598	62	(Rubinos and Barral 2013)	Spain	3.69
RM	225	219	5	(Somlai et al. 2008)	Hungary	1.85
RM	568	392	101	(Somlai et al. 2008)	Hungary	3.89
Silica fume (SF)	2	3	100	(Puertas et al. 2015)	Spain	14
SF	1	2	92	(Puertas et al. 2015)	Spain	11
SF	1	0	870	(Gökçe et al. 2020)	Turkey	68
SF	33	24	540	(Sahoo et al. 2007)	India	109
SF	4	6	297	(Singovszka et al. 2017)	Slovakia	35
SF	0	0	100	(Alonso et al. 2020)	Slovakia	8
SF	0	0	92	(Alonso et al. 2020)	Slovakia	7
Steel slag (SS)	5	0	1	(Puch et al. 2005)	Germany	5
SS	23	21	0	(Alonso et al. 2020)	Germany	53

Table 1 (continued)

Literature						Evaluation
SS	23	15	4	(Alonso et al. 2020)	Germany	45
SS	16	20	0	(Alonso et al. 2020)	Germany	45
SS	20	16	0	(Alonso et al. 2020)	Germany	43
SS	62	21	51	(Schroeyers et al. 2018)	EU MS	96
SS	23	15	51	(Schroeyers et al. 2018)	EU MS	48
SS	13	7	21	(Schroeyers et al. 2018)	EU MS	25
SS	25	5	10	(Schroeyers et al. 2018)	EU MS	33
SS	196	30	148	(Schroeyers et al. 2018)	EU MS	250
SS	0	150	0	(Schroeyers et al. 2018)	EU MS	215
SS	88	49	0	(Schroeyers et al. 2018)	EU MS	158
Volcanic ash (VA)	59	132	1130	(Turhan 2008)	Turkey	335
VA	92	138	1200	(Righi and Bruzzi 2006)	Turkey	382
VA	190	210	1900	(Righi and Bruzzi 2006)	Greece	637
VA	280	270	1900	(Righi and Bruzzi 2006)	Greece	812
Waste glass powder (WP)	8	11	227	(Puertas et al. 2015)	Spain	41
WP	9	11	2	(Alonso et al. 2020)	Spain	25
EC (1999a)	40	30	400			370
UNSCEAR 1993, 2000)	33	45	420			370

Deep neural networks (DNN)

Currently, the backpropagation approach is used to train the multilayer perceptron, the most popular type of neural network (Martin et al. 2014). In terms of performance, multiple-layer networks outperform single-layer networks. For instance, a two-layer network can be trained to mimic most functions accurately using a two-layer sigmoid. However, this cannot be achieved with a single-layer network (Martin et al. 2014). Typically, two or three hidden layers are adequate in practical neural networks. Using four or more layers is unusual (Panchal et al. 2011; Martin et al. 2014; Uzair and Jamil 2020). Research on DNN's optimizers (LM, SCG, and BR) (Oyebisi et al. 2023d) and 2–4 hidden layers (Raheem et al. 2023; Oyebisi and Alomayri 2023b; Oyebisi et al. 2023b; Ekwueme 2024a) showed that LM with 3 hidden layers had the best performance metrics compared to other optimizers and hidden layers. Thus, this study employed a 3-hidden layer network of 5–30 nodes per layer, and the rectified linear unit (ReLU) activation function was used.

Model training and testing

MATLAB R2021a was used to develop a function that loaded the non-parametric data (training and target datasets). The target dataset contained Ra_{eq} values, whereas the training datasets included ^{226}Ra, ^{232}Th, and ^{40}K results. With LM ('trainlm') as the learning algorithm, the network was trained using training and target datasets. The network comprises 3 hidden layers and 5–30 nodes in each layer to ascertain the influence of different neurons on DNN topology and select the optimal DNN structure for forecasting the material's Ra_{eq}. This configuration uses the first network's output as the second network's input and the second network's output as the third network's input (Martin et al. 2014). This indicates that a layer's output becomes the input for the layer after it is in a multilayer network. Equation (2) explains this process (Martin et al. 2014). There may be variations in the transfer function and the total number of neurons in each layer. Equation (3) thus displays the third network's output (Martin et al. 2014).

$$a^{m+1} = f^{m+1}\left(W^{m+1}a^{m} + b^{m+1}\right) \mathit{for}\ m = 0,1,\ldots,M-1$$

$$a^{3} = f^{3}\left(W^{3}f^{2}\left(W^{2}f^{1}\left(W^{1}p + b^{1}\right) + b^{2} + b^{3}\right)\right.$$

The neurons in the first layer receive inputs from outside sources, as per Eq. (5). This provides the initial value for Eq. (4).

$$a^{0} = p$$

The outputs of the neurons in the final layer, as indicated by Eq. (4), are known as the network outputs.

$$a = a^{M}$$

where $a, f, m, p, W, and\ b$ represent the output vector, transfer function, network layers, input vector, weight matrix, and bias vector.

The DNN model can be prone to overfitting due to the additional classes of abstraction that enable rare-dependent training of datasets (Ly et al. 2021a). For this reason, a random stream or arbitrary value (491218362) was applied to prevent overfitting (Oyebisi and Alomayri 2023c; Oyebisi et al. 2023a; Ekwueme 2024b). Additionally, this stream guarantees that the network always produces the same output after training (Ly et al. 2021b). The influence of outliers on the DNN model was reduced by identifying and removing them from the dataset, treating them as missing values.

Table 1 shows that 860 datasets were acquired, comprising 215 data each for ^{226}Ra, ^{232}Th, ^{40}K, and Ra_{eq}. The DNN was learned with 760 datasets, comprising 190-trained data each for ^{226}Ra, ^{232}Th, ^{40}K, and Ra_{eq}, while the model's accuracy was confirmed with 25-untrained data. Training, validation, and testing comprised 70, 15, and 15% of the learning datasets. Ultimately, the relation shown in Eq. (6) was used to train the network:

$$[P,\ R] = t[X,\ Y\prime,\ Z\prime]$$

where P, R, t, X, Y, *and* Z connote predictor, record, train, network, training dataset, and target dataset.

Validation of developed models

The accuracy of the developed models was validated by 25 analytical datasets (non-parametric data) each for ^{226}Ra, ^{232}Th, ^{40}K, and Ra_{eq}. The datasets were randomly selected and spanned the entire spectrum of conditions.

Evaluation of performance metrics

Performance metrics evaluate the precision of the developed model. Consequently, the model's precision was verified using R (correlation coefficient), R^2 (coefficient of determination), MSE (mean square error), and RMSE (root mean square error). These are illustrated in Eqs. (7), 8, 9 and 10). Mathematically, DNN models are more accurate when R and R^2 values are around 1 and MSE and RMSE values are around 0. Besides, performance, training state, histogram, and regression outputs were plotted. Equations (11) and (12) were used to validate the developed DNN. Figure 2 shows the graphical representation of the best network architecture, depicting 3 input variables (scaling layer), 3 hidden layers with 15 nodes in each layer (perceptron layers), and an output variable (bounding layer). Figure 3 displays the DNN flowchart procedure.

$$R = 1 - \frac{\sum_{i=1}^{n}\left(y_i^{pred} - y_i^{true}\right)}{\sum_{i=1}^{n}\left(y_i^{pred} - \bar{y}_i^{true}\right)}$$

$$R^2 = 1 - \frac{\sum_{i=1}^{n}\left(y_i^{pred} - y_i^{true}\right)^2}{\sum_{i=1}^{n}\left(y_i^{pred} - \overline{y^{true}}\right)^2}$$

$$MSE = \frac{1}{n}\sum_{i=1}^{n}\left(y_i^{pred} - y_i^{true}\right)^2$$

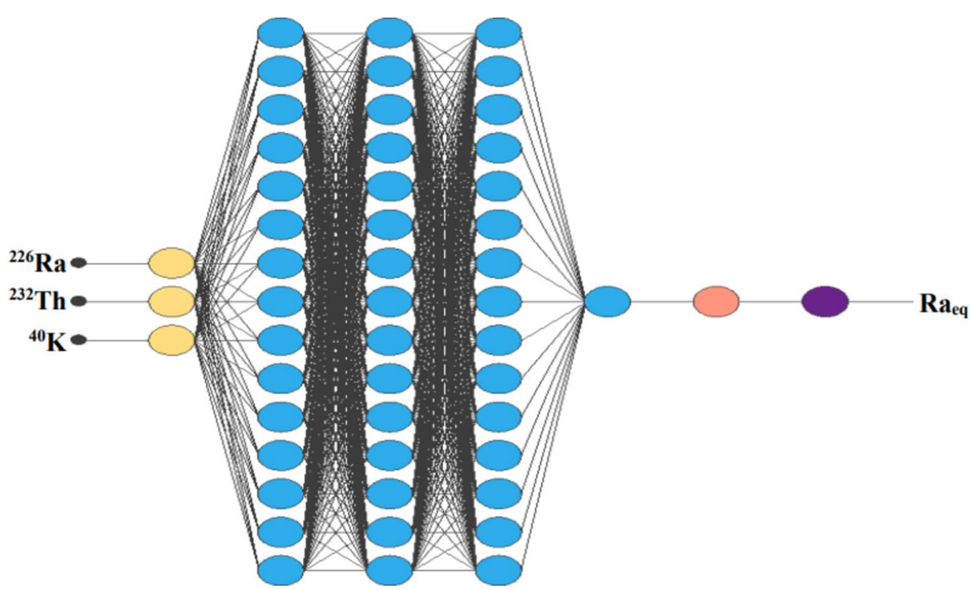

Fig. 2 Graphical representation of the best DNN architectures for Ra_{eq} (3–15-15-15-1)

$$RMSE = \sqrt{\frac{1}{n}\sum_{i=1}^{n}(y_i^{pred} - y_i^{true})^2}$$

$$function\,[CS,\ FS,\ or\ STS] = n[P,\ D]$$

$$CS,\ FS,\ or\ STS = P\left(D'\right)$$

where *n and D represent the test network and data.*

Sensitivity analysis

Understanding the factors that have a major impact on model estimates is essential. This was accomplished by computing the derivatives of a model's outputs with regard to its inputs. In cases where poor model formulation is not expected to be a significant problem, sensitivity analyses are a helpful technique for estimating the potential significance of model parameters as sources of uncertainty in model predictions (Hamby 1994). Machine learning requires numerous tests to evaluate

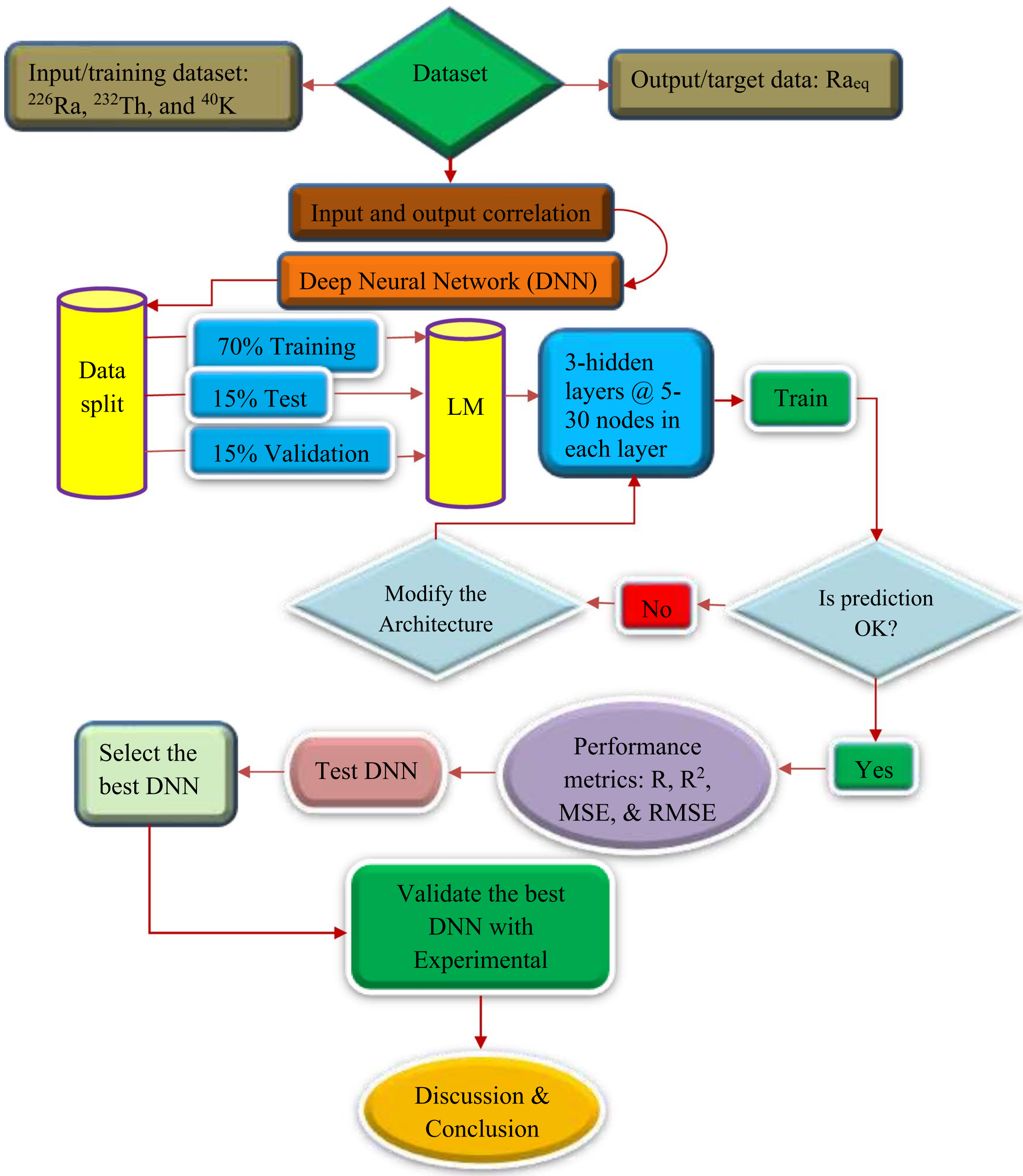

Fig. 3 DNN's flowchart

and confirm the quality and dependability of the created model on a range of data sets. Improvements in the prediction model's accuracy and efficacy throughout training, testing, and validation of available data sets may not imply or promise improved performance in the end (Alabi et al. 2023). Sensitivity analysis (SA), as illustrated in Eq. (133), was used to determine the relative significance of the variables that explained the output (Ra_{eq}). High derivative values suggest greater significance, while values close to 0 indicate lesser significance (Hamby 1994; Khan et al. 2022).

$$SA = \frac{Range_{\ output}}{\sum_{i=1}^{p} Range_{\ output}}$$

$$whereRange_{output} = Max\left(\bar{x}_{output}\right) - Min\left(\bar{x}_{output}\right).$$

Results and discussion

Statistical datasets

Table 2 summarizes the statistical analysis of the activity concentration of radionuclides and the computed results of Ra_{eq} of recycled waste materials. From Table 2, the ^{226}Ra, ^{232}Th, ^{40}K, and Ra_{eq} varied from 0 to 1135, 0–1350, 0–1900, and 0.58–1370 Bq kg^{-1} with mean values of 174 ± 15, 112 ± 14, and 362 ± 26 Bq kg^{-1}, respectively. The distribution of Ra_{eq} varied among the materials studied, showing a mean value of 231 ± 18 Bq kg^{-1} and a range between 0.58 and 1370 Bq kg^{-1}. Red mud had the lowest Ra_{eq}, whereas FA showed the most significant value. The variations in the activity concentration of radionuclides and Ra_{eq} can be explained by the fact that the waste materials used to produce these recycled products have varying mineral compositions. Hence, the concentration of natural radioactivity varies depending on the geological composition, kind of material, origin, and metallurgical operations (Kovler 2011; Fidanchevski et al. 2021b). In addition to other chemical and physical changes that occur during the production processes, removing organic materials and moisture from ash and shells would cause the enrichment and redistribution of activity concentrations. This indicates an uneven distribution of natural radioactivity in raw materials. However, the activity concentration of radionuclides in most of the surveyed materials was within the globally recommended ranges of building materials, which are 16–70, 11–64, and 140–850 Bq kg^{-1} for ^{226}Ra, ^{232}Th, and ^{40}K (UNSCEAR 2000). A range of 49–240, 30–190, and 400–1600 Bq kg^{-1} for ^{226}Ra, ^{232}Th, and ^{40}K, respectively (EC 1999b) and maximum recommendations of 40, 190, and 1570 Bq kg^{-1} for ^{226}Ra, ^{232}Th, and ^{40}K, respectively (International Atomic Energy Agency 2014). Most of the surveyed RWMs met the 370 Bq kg^{-1} maximum permissible recommendation for building materials stipulated by UNSCEAR (2000) and EC (1999a). These findings indicated that, with appropriate screening and precautions, the surveyed materials can be utilized both as building and construction materials.

Input-output response

The responses of activity concentration of radionuclides to the target radionuclide (Ra_{eq}) are indicated in Fig. 4. Figure 4 (a) shows an increase in Ra_{eq} with increasing ^{226}Ra with R^2 of 0.5083, yielding a good response. This is because the radium content in any material is directly proportional to the Ra_{eq}. Radium activity equivalent assumes that the activity concentration of a radionuclide is equivalent to 370 Bq kg^{-1} of ^{226}Ra, which gives an absorbed dose rate of 1.5 mGy (1 mSv) per year (UNSCEAR 2000). A similar trend was obtained for the ^{40}K isotope in Fig. 4 (b) in that an increase in ^{40}K concentration increases the Ra_{eq}; however, the R-value was approximately 18%, indicating a poor response. Figure 4 (c) depicts a decrease in Ra_{eq} with increasing ^{232}Th concentration. Thus, Fig. 4 (a)-(c) reveal that the most significant contribution to the Ra_{eq} of surveyed RWMs comes from ^{226}Ra concentration.

Sensitivity analysis

Figure 5 shows the impact of each input variable on the modelling of radium activity equivalent of RWMs. The input variables significantly influence the outcome projection. According to the analysis, ^{226}Ra is the most relevant factor in the degree of significance, contributing 47.42% to the model's development. The ^{232}Th came second with a percentage contribution of 41.90%, while isotope of ^{40}K was less significant, contributing 10.68% to the modelling of radium activity equivalent. This aligns with the response results between the input and target variables in Fig. 4. Figure 4 shows an increase in Ra_{eq} with increasing ^{226}Ra

Table 2 Statistical analysis of non-parametric datasets

Variable	Unit	Minimum	Maximum	Mean	Median	StDev	Factor
^{226}Ra	Bq kg^{-1}	0	1135	173.72	97.5	207.64	Input
^{232}Th	Bq kg^{-1}	0	1350	112.40	50	194.12	Input
^{40}K	Bq kg^{-1}	0	1900	361.84	240	362.33	Input
Ra_{eq}	Bq kg^{-1}	0.58	1370	231.28	177	246.72	Output

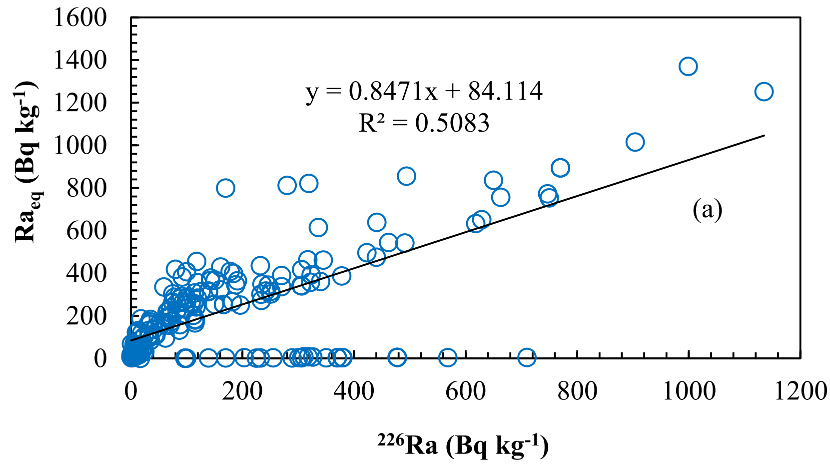

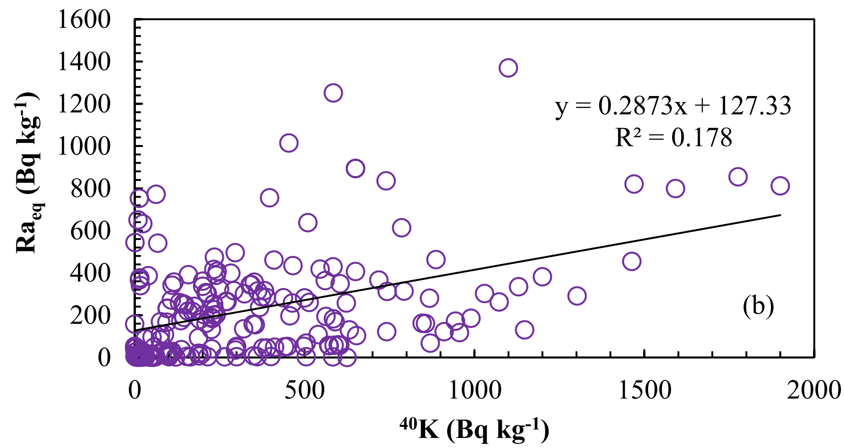

Fig. 4 Input-output response

concentration and ^{40}K isotope. Nonetheless, the sensitivity analysis results were dependent on the quantity of input variables and data points utilized to train the model. Each variable is influenced by ML approaches (Ahmad et al. 2021). Therefore, various results are produced when additional input variables are introduced, and the proportions of the activity concentration of radionuclides are changed.

Performance metrics of DNN structures

Table 3 shows the neural network performance metrics used in the DNN's training, validation, and testing of variables. For all network structures, the MSE, RMSE, R, and R^2 values proved and supported the validity and flexibility of the model. As the number of neurons in the hidden layers increased, the results

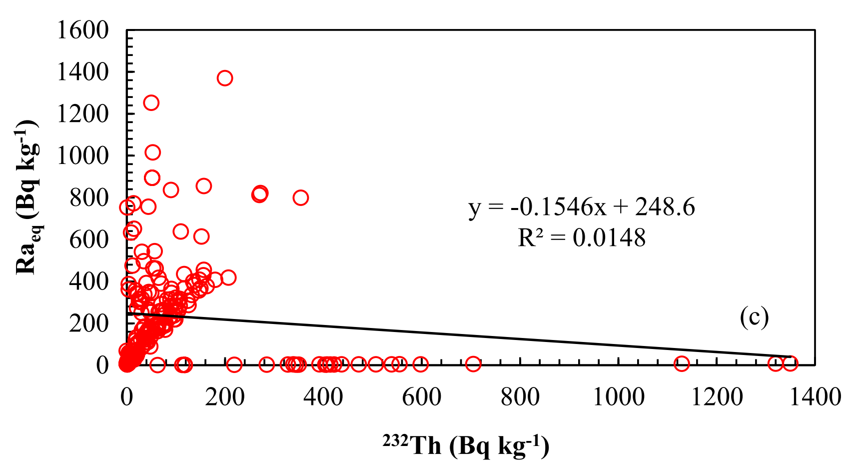

Fig. 4 (continued)

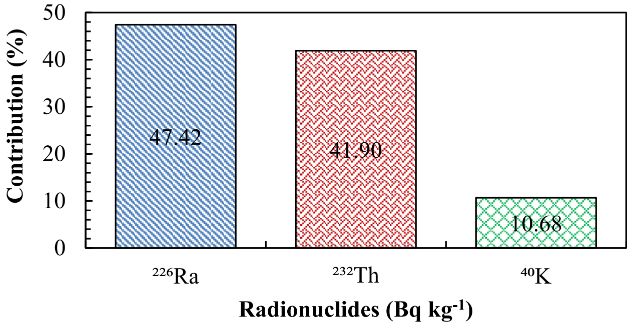

Fig. 5 Sensitivity report

from Table 2 demonstrated a performance improvement, which is consistent with other studies (Shafi et al. 2006; Oyebisi and Alomayri 2023b). The 3–15-15-15-1 network architecture, as indicated in Table 3, outperformed other structures for training, validating, and testing the Ra_{eq} model with the least MSE and RMSE. The MSE performance indicator of the 3–15-15-15-1 network structure for modelling the Ra_{eq} of surveyed RMWs was about 100% lower than other network structures. Strong correlation of R and R^2 values with 0.9969 and 0.9985 for training, 0.9591 and 0.9791 for validation, and 0.9868 and 0.9934 for testing in Fig. 6 corroborate the best performance metrics exhibited by 3–15-15-15-1 network structure. Strong correlation and accuracy of the model are indicated by lower values of the errors (MSE and RMSE) and higher values of the coefficients (R and R^2) (Willmott and Matsuura 2005). Thus, it is clear from Table 3 that training, validating, and testing Ra_{eq} datasets using a 3-hidden layer with 15 nodes per layer allowed the datasets to reach their optimal learning structures and produce optimal performance metrics. These findings can be associated with the generalization abilities of several layers, enabling them to learn all features between the input and target variables and perform advanced categorization.

Figure 7 shows the direction and intensity of the linear correlations between the target and expected parameters. With strong correlation coefficients of 0.95914 shown in Fig. 7, the developed DNN structures can predict the Ra_{eq} of RMWs and are judged to be dependable, accurate, and outstandingly performed.

Validation of developed DNN architectures

The validation process employed raw datasets from the experimental works to further demonstrate the capabilities of the 3–15-15-15-1 network structures. The correlation between the actual and anticipated strengths is shown in Table 4, along with the corresponding absolute errors (AB), relative errors (RE), absolute uncertainty, relative uncertainty, and percentage uncertainty. Figure 8 presents the verification of predicted radium activity equivalent against analytical results. Therefore, the created DNN models learned and accurately predicted the experimental data with 0.9996 R^2. This further suggests that given the model parameters of

Table 3 Neural network performance metrics for various DNN architectures

Architecture	3–5-5-5-1	3–10-10-10-1	3–15-15-15-1	3–20-20-20-1	3–25-25-25-1	3–30-30-30-1
MSE	0.3157	0.7137	0.0001	1	0.8561	0.2673
RMSE	0.5619	0.8448	0.0010	1	0.9253	0.5170

Fig. 6 Performance indicators for DNN architectures

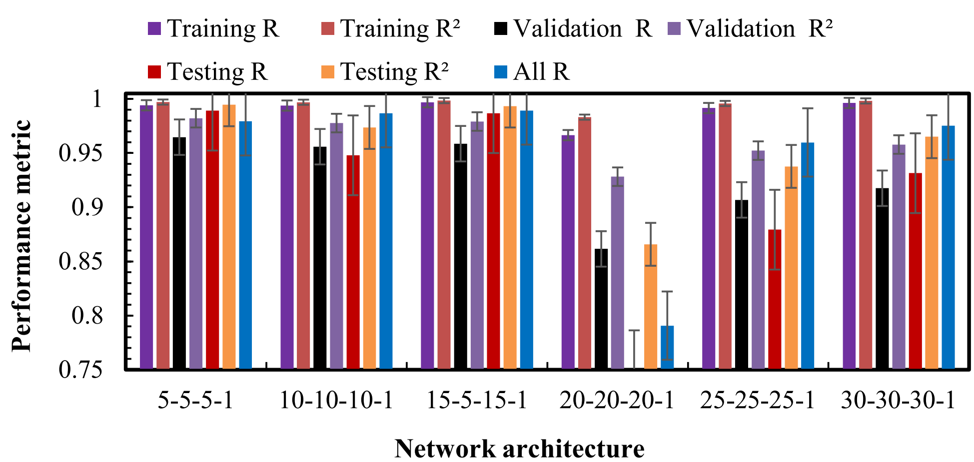

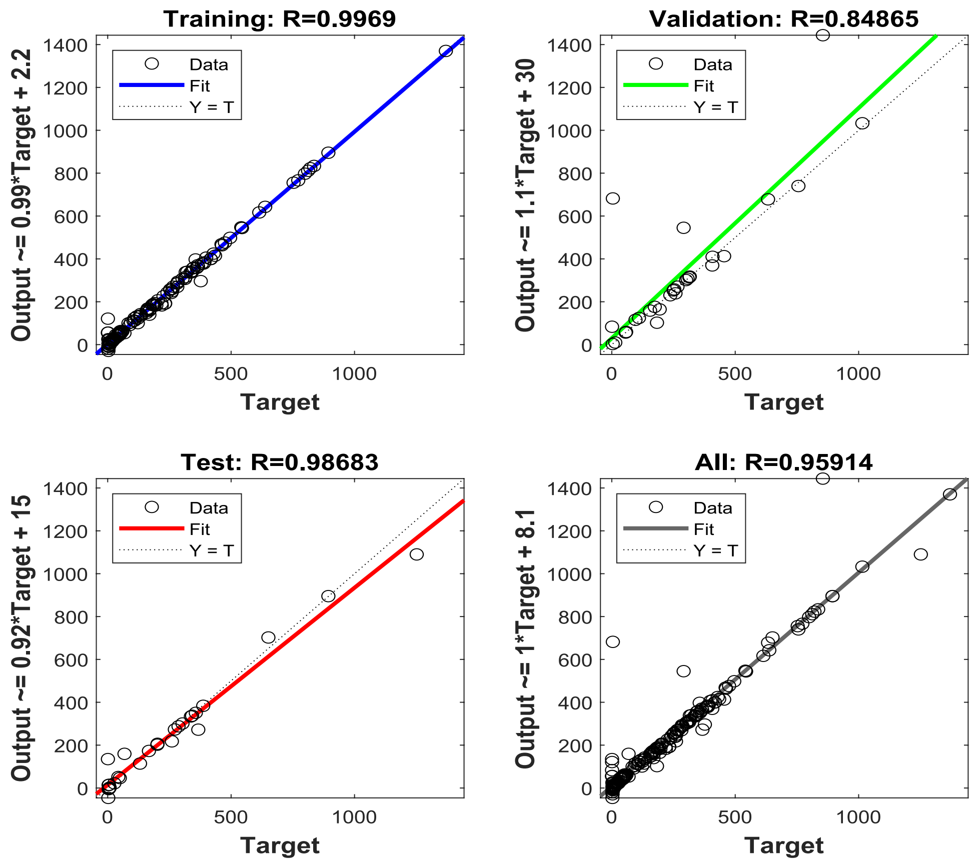

Fig. 7 Regression plots for the best DNN model (3–15-15-15-1)

the activity concentration of radionuclides, the developed DNN model can reproduce the analytical results with high accuracy. Additionally, the suggested model can understand the relationship between various activity concentrations of radionuclides and the responses.

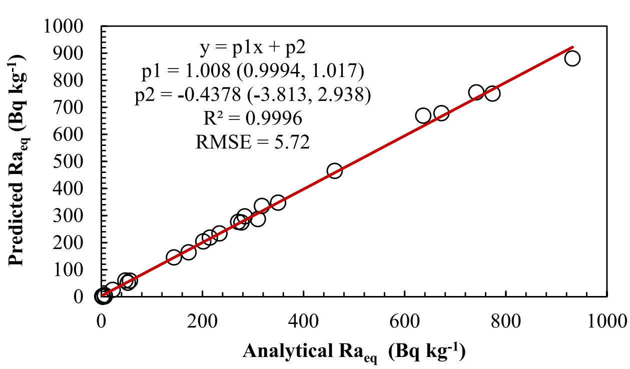

Fig. 8 Relationship between the predicted and analytical Ra_{eq}

The predicted Ra_{eq} of RWMs with 3–15-15-15-1 network architecture, as shown in Table 4, exhibited variance within -24.58 and $+99.71\%$ for validating the developed DNN structures. This variance is due to an extensive range of activity concentration of radionuclides, which is permissible with the international recommendations. From Table 4, the predicted Ra_{eq} could differ from the analytical Ra_{eq} with 2 ± 1 Bq kg^{-1} (absolute uncertainty), yielding a sense of $2 \pm 1\%$ difference (percentage uncertainty). Thus, a 3–15-15-15-1 network structure is suitable and accurate.

Conclusions

This study assesses the non-parametric data of activity concentrations and develops the DNN-based model to evaluate and forecast the Ra_{eq} of RWMs (target variable) with ^{226}Ra, ^{232}Th, and ^{40}K as input variables. Based on the findings of this investigation, RHA, MS, POC, POFA, ISSA, LS, MP, NS, PA, RM, SF, SS, and WP pose no risk to Ra_{eq}. However, owing to provenance, about 31, 100, 31, 20, 18, 13, 50, 34,

Table 4 Validation of untrained datasets with 3–15-15-15-1 structure

	Radionuclide (Bq kg^{-1})			Ra_{eq} (Bq kg^{-1})		Error	
Uncertainty	^{226}Ra	^{232}Th	^{40}K	Analytical	Predicted	AE	RE (%)
	9.80	5.70	69.80	23	25.20	−2.20	−9.57
	6.90	4.63	571	57	58.70	−1.70	−2.98
	8.75	7.98	421	53	51.30	1.70	3.21
	62	53	457	173	163.80	9.20	5.32
	541	102	714	742	755	−13.00	−1.75
	317	54	886	462	464.80	−2.80	−0.61
	99	113	309	284	296.70	−12.70	−4.47
	263	49	216	350	347.30	2.70	0.77
	825	53	402	932	880	52.00	5.58
	179	55	172	271	276.20	−5.20	−1.92
	128	45	119	202	203.90	−1.90	−0.94
	89	140	378	318	335	−17.00	−5.35
	55	41	398	144	144.8	−0.80	−0.56
	378	154	2285	774	750	24.00	3.10
	125	92	695	310	286.7	23.30	7.52
	1	3	25	7	5.98	1.02	14.57
	410	182	34	673	678	−5.00	−0.74
	209	17	3	234	233.6	0.40	0.17
	165	328	53	2.21	1.79	0.42	19.00
	347	283	48	2.59	0.01	2.58	99.61
	210	539	112	3.43	0.01	3.42	99.71
	0	0	92	7	0.8	6.20	88.57
	23	15	51	48	59.8	−11.80	−24.58
	0	150	0	215	218	−3.00	−1.40
	190	210	1900	637	668.5	−31.50	−4.95
Absolute uncertainty (Bq kg^{-1})	128 ± 40	54 ± 25	216 ± 113	215 ± 56	218 ± 55	-	-
Relative uncertainty	0.31	0.46	0.52	0.26	0.25	-	-
Percentage uncertainty (%)	128 ± 31	54 ± 46	216 ± 52	215 ± 26	218 ± 25	-	-

25, and 75% of BA, CS, FA, GGBFS, GWP, MK, MT, PG, PM, and VA entries surpassed the permissible limit of 370 Bq kg^{-1}. All input variables impact the Ra_{eq} of RWMs, with ^{226}Ra concentration contributing the most significant impact to the Ra_{eq}, accounting for about 47%. This is followed by ^{232}Th concentration and ^{40}K isotope in the order of about 42 and 11%. Moreover, the 8–15-15-15-1 network architecture demonstrated the best prediction accuracy in forecasting the Ra_{eq} of RWMs with about a 100% reduction in MSE compared to other network structures. With the developed DNN structure, the predicted Ra_{eq} exhibited a strong correlation with the analytical Ra_{eq}, yielding 0.9996 R^2.

This study filled this knowledge gap and demonstrated the viability of DNN in forecasting the Ra_{eq} of RWMs in relation to the activity concentration of radionuclides. Besides, this study reported the importance of each radionuclide to the Ra_{eq} of RWMs, educating the potential users about the radiological risk.

Recommendations for future studies

Additional study is necessary by adding more input factors to the radiological indexes of other RWMs. Increasing the amount of variables helps the models become more accurate and responsive. In addition, parametric test analysis of datasets could be explored, requiring data to fit a specific pattern or distribution. The parametric analysis should also incorporate measurement uncertainty, such as standard uncertainty linked to the estimate, measurand's probability distribution, and the measurand's coverage interval for a certain coverage probability to provide a quantitative expression of confidence in the results.

Author contributions S.O. conceptualized and designed the study; S.O., M.I.S., P.J., H.O., and M.O.O. collected the data; S.O. analyzed and interpreted the results; S.O. analyzed the data with software, and S.O. wrote the manuscript in consultation with M.I.S., P.J., H.O., and M.O.O. All authors reviewed the manuscript.

Funding The authors declare that no funds, grants, or other support were received during the preparation of this manuscript.

Data availability The statement of code generation is freely accessible through open access in the Zenodo Repository at https://doi.org/10.5281/zenodo.11097036.https://doi.org/10.5281/zenodo.11097036

Declarations

Competing interests The authors declare no competing interests.

Statement of code generation The statement of code generation is freely accessible through open access in the Zenodo Repository at https://doi.org/10.5281/zenodo.11097036.

References

Adagunodo TA, George AI, Ojoawo IA et al (2018) Radioactivity and radiological hazards from a kaolin mining field in Ifonyintedo, Nigeria. MethodsX 5:362–374. https://doi.org/10.1016/j.mex.2018.04.009

Ademola JA, Onyema UC (2014) Assessment of Natural radionuclides in fly Ash produced at Orji River Thermal Power Station, Nigeria and the Associated Radiological Impact. Nat Sci (Irvine) 06:752–759. https://doi.org/10.4236/ns.2014.610075

Ahmad W, Ahmad A, Ostrowski KA et al (2021) Application of Advanced Machine Learning approaches to predict the compressive strength of concrete containing supplementary Cementitious materials. Materials 14:5762. https://doi.org/10.3390/ma14195762

Alabi SA, Arum C, Adewuyi AP et al (2023) Mathematical model for prediction of compressive strength of ternary blended cement concrete utilizing gene expression programming. Sci Afr 22:e01954. https://doi.org/10.1016/j.sciaf.2023.e01954

Alam MN, Chowdhury MI, Kamal M et al (2000) Radionuclide concentrations in mussels collected from the southern coast of Bangladesh. J Environ Radioact 47:201–212. https://doi.org/10.1016/S0265-931X(99)00038-7

Alonso MM, Pasko A, Gascó C et al (2018) Radioactivity and pb and ni immobilization in SCM-bearing alkali-activated matrices. Constr Build Mater 159:745–754. https://doi.org/10.1016/j.conbuildmat.2017.11.119

Alonso MM, Suárez-Navarro JA, Pérez-Sanz R et al (2020) Data on natural radionuclide's activity concentration of cement-based materials. Data Brief 33:106488. https://doi.org/10.1016/j.dib.2020.106488

Amin YM, Uddin Khandaker M, Shyen AKS et al (2013) Radionuclide emissions from a coal-fired power plant. Appl Radiat Isot 80:109–116. https://doi.org/10.1016/j.apradiso.2013.06.014

Beretka J, Mathew PJ (1985) Natural radioactivity of Australian building materials, Industrial Wastes and By-products. Health Phys 48:87–95. https://doi.org/10.1097/00004032-198501000-00007

Chinchón-Payá S, Piedecausa B, Hurtado S et al (2011) Radiological impact of cement, concrete and admixtures in Spain. Radiat Meas 46:734–735. https://doi.org/10.1016/j.radmeas.2011.06.020

Council of European Union (2014) Council Directive 2013/59/Euratom of 5 December 2013 laying down basic safety standards for protection against the dangers arising from exposure to ionizing radiation, and repealing directives 89/618/Euratom, 90/641/Euratom, 96/29/Euratom, 97/43/Euratom and 2003/122/Euratom. Off. J. Eur, United Nation

Ekwueme BN (2024a) Deep neural network modeling of river discharge in a tropical humid watershed. Earth Sci Inf. https://doi.org/10.1007/s12145-023-01219-w

Ekwueme BN (2024b) Deep neural network modeling of river discharge in a tropical humid watershed. Earth Sci Inf. https://doi.org/10.1007/s12145-023-01219-w

El Arabi AM, Ahmed NK, Salahel Din K (2007) Assessment of terrestrial gamma radiation doses for some Egyptian granite samples. Radiat Prot Dosimetry 128:382–385. https://doi.org/10.1093/rpd/ncm367

European Commission (1999a) Radiological protection principles concerning the natural radioactivity of building materials, Radiation Protection Report -RP-112. Luxembourg

European Commission (1999b) Radiological protection principles concerning the natural radioactivity of building materials, Radiation Protection Report -RP-112. Luxembourg

Feng T, Lu X (2016) Natural radioactivity, radon exhalation rate and radiation dose of fly ash used as building materials in Xiangyang, China. Indoor Built Environ 25:626–634. https://doi.org/10.1177/1420326X15573276

Fidanchevski E, Angjusheva B, Jovanov V et al (2021a) Technical and radiological characterisation of fly ash and bottom ash from thermal power plant. J Radioanal Nucl Chem 330:685–694. https://doi.org/10.1007/s10967-021-07980-w

Gallyas M, Török I (1984) Natural radioactivity of raw materials and products in the Cement Industry. Radiat Prot Dosimetry 7:69–71. https://doi.org/10.1093/oxfordjournals.rpd.a082965

Gezer F, Turhan Ş, Uğur FA et al (2012) Natural radionuclide content of disposed phosphogypsum as TENORM produced from phosphorus fertilizer industry in Turkey. Ann Nucl Energy 50:33–37. https://doi.org/10.1016/j.anucene.2012.07.018

Gökçe HS, Canbaz Öztürk B, Çam NF, Andiç-Çakır Ö (2020) Natural radioactivity of barite concrete shields containing commonly used supplementary materials. Constr Build Mater 236:117569. https://doi.org/10.1016/j.conbuildmat.2019.117569

Gupta M, Mahur AK, Varshney R et al (2013) Measurement of natural radioactivity and radon exhalation rate in fly ash samples from a thermal power plant and estimation of radiation doses. Radiat Meas 50:160–165. https://doi.org/10.1016/j.radmeas.2012.03.015

Hamby DM (1994) A review of techniques for parameter sensitivity analysis of environmental models. Environ Monit Assess 32:135–154. https://doi.org/10.1007/BF00547132

Harb S, El-Kamel AH, Abd El-Mageed AI et al (2008) Concentration of U-238, U-235, Ra-226, Th-232 and K-40 for some granite samples in eastern desert of Egypt. In: Proc. Third Environ. Phys. Conf. Aswan, Egypt, p 335

Hassan NM, Ishikawa T, Hosoda M et al (2010) Assessment of the natural radioactivity using two techniques for the measurement of radionuclide concentration in building materials used in Japan. J Radioanal Nucl Chem 283:15–21. https://doi.org/10.1007/s10967-009-0050-6

Ignjatović I, Sas Z, Dragaš J et al (2017) Radiological and material characterization of high volume fly ash concrete. J Environ Radioact 168:38–45. https://doi.org/10.1016/j.jenvrad.2016.06.021

International Atomic Energy Agency (2014) Radiation Protection and Safety of Radiation sources. International Basic Safety Standards, Vienna

Kamunda C, Mathuthu M, Madhuku M (2016) An Assessment of Radiological hazards from Gold Mine tailings in the Province of Gauteng in South Africa. Int J Environ Res Public Health 13:138. https://doi.org/10.3390/ijerph13010138

Karangelos DJ, Petropoulos NP, Anagnostakis MJ et al (2004) Radiological characteristics and investigation of the radioactive equilibrium in

the ashes produced in lignite-fired power plants. J Environ Radioact 77:233–246. https://doi.org/10.1016/j.jenvrad.2004.03.009
Karim MR, Khandaker MU, Asaduzzaman K et al (2019) Radiological risks assessment of building materials ingredients: Palm oil clinker and fuel ash. Indoor Built Environ 28:479–491. https://doi.org/10.1177/1420326X18776705
Khan IU, Sun W, Lewis E (2020) Review of low-level background radioactivity studies conducted from 2000 to date in people Republic of China. J Radiat Res Appl Sci 13:406–415. https://doi.org/10.1080/16878507.2020.1744330
Khan K, Salami BA, Jamal A et al (2022) Prediction models for estimating compressive strength of concrete made of manufactured sand using gene expression programming model. Materials 15:5823. https://doi.org/10.3390/ma15175823
Khandaker MU, Asaduzzaman K, Sulaiman AF, Bin et al (2018) Elevated concentrations of naturally occurring radionuclides in heavy mineral-rich beach sands of Langkawi Island, Malaysia. Mar Pollut Bull 127:654–663. https://doi.org/10.1016/j.marpolbul.2017.12.055
Kobeissi MA, El-Samad O, Rachidi I (2013) Health assessment of natural radioactivity and radon exhalation rate in granites used as buildingmaterials in Lebanon. Radiat Prot Dosimetry 153:342–351. https://doi.org/10.1093/rpd/ncs110
Kocsis E, Tóth-Bodrogi E, Peka A et al (2021) Radiological impact assessment of different building material additives. J Radioanal Nucl Chem 330:1517–1526. https://doi.org/10.1007/s10967-021-07897-4
Kovler K (2011) Legislative aspects of radiation hazards from both gamma emitters and radon exhalation of concrete containing coal fly ash. Constr Build Mater 25:3404–3409. https://doi.org/10.1016/j.conbuildmat.2011.03.031
Kovler K (2012) Radioactive materials. Toxicity of building materials. Elsevier, pp 196–240
Krmpotić M, Rožmarić M, Barišić D (2015) Mussels (Mytilus galloprovincialis) as a bio-indicator species in radioactivity monitoring of Eastern Adriatic coastal waters. J Environ Radioact 144:47–51. https://doi.org/10.1016/j.jenvrad.2015.02.027
Krstić D, Nikezić D, Stevanović N, Vučić D (2007) Radioactivity of some domestic and imported building materials from South Eastern Europe. Radiat Meas 42:1731–1736. https://doi.org/10.1016/j.radmeas.2007.09.001
Kumar V, Ramachandran TV, Prasad R (1999) Natural radioactivity of Indian building materials and by-products. Appl Radiat Isot 51:93–96. https://doi.org/10.1016/S0969-8043(98)00154-7
Lehmann R (1996) Strahlenbelastung Durch nat€urliche radionuklide in baumaterialien, fossilen brennstoffen und Dungemitteln. Bundesamt fur Strahlenshutz, Berlin
Lu X, Li LY, Wang F et al (2012) Radiological hazards of coal and ash samples collected from Xi'an coal-fired power plants of China. Environ Earth Sci 66:1925–1932. https://doi.org/10.1007/s12665-011-1417-x
Ly H-B, Nguyen T-A, Thi Mai H-V, Tran VQ (2021a) Development of deep neural network model to predict the compressive strength of rubber concrete. Constr Build Mater 301:124081. https://doi.org/10.1016/j.conbuildmat.2021.124081
Mahur AK, Kumar R, Sengupta D, Prasad R (2008) Estimation of radon exhalation rate, natural radioactivity and radiation doses in fly ash samples from Durgapur thermal power plant, West Bengal, India. J Environ Radioact 99:1289–1293. https://doi.org/10.1016/j.jenvrad.2008.03.010
Martin H, Howard D, Mark B, Orlando DJ (2014) Neural Network Design, 2nd edn. Martin Hagan, Oklahoma
Mishra UC (2004) Environmental impact of coal industry and thermal power plants in India. J Environ Radioact 72:35–40. https://doi.org/10.1016/S0265-931X(03)00183-8
Msila X, Labuschagne F, Barnard W, Billing DG (2016) Radioactive nuclides in phosphogypsum from the lowveld region of South Africa. S Afr J Sci 112:5. https://doi.org/10.17159/sajs.2016/20150102
Mustonen R (1984) Natural radioactivity in and Radon Exhalation from Finnish Building materials. Health Phys 46:1195–1203. https://doi.org/10.1097/00004032-198406000-00003
Nuccetelli C, Pontikes Y, Leonardi F, Trevisi R (2015) New perspectives and issues arising from the introduction of (NORM) residues in building materials: a critical assessment on the radiological behaviour. Constr Build Mater 82:323–331. https://doi.org/10.1016/j.conbuildmat.2015.01.069
Okeji MC, Agwu KK, Idigo FU (2012) Assessment of natural radioactivity in phosphate Ore, Phosphogypsum and Soil samples around a phosphate fertilizer plant in Nigeria. Bull Environ Contam Toxicol 89:1078–1081. https://doi.org/10.1007/s00128-012-0811-8
Oyebisi S, Alomayri T (2023a) Potential application of artificial intelligence to the alpha and gamma radiation from agricultural byproducts used as building and construction materials. Sci Afr 21:e01792. https://doi.org/10.1016/j.sciaf.2023.e01792
Oyebisi S, Alomayri T (2023b) Artificial intelligence-based prediction of strengths of slag-ash-based geopolymer concrete using deep neural networks. Constr Build Mater 400:132606. https://doi.org/10.1016/j.conbuildmat.2023.132606
Oyebisi S, Owamah H (2023) Application of machine learning techniques in the prediction of excess lifetime cancer risks of agricultural byproducts used as building and construction materials. Clean Waste Syst 5:100088. https://doi.org/10.1016/j.clwas.2023.100088
Oyebisi S, Igba T, Olutoge F, Ede A (2023a) Application of artificial intelligence in the hazard indexes of recycled agricultural waste materials. Multiscale Multidisciplinary Model Experiments Des. https://doi.org/10.1007/s41939-023-00327-w
Oyebisi S, Igba T, Olutoge F, Ede A (2023b) Application of artificial intelligence in the hazard indexes of recycled agricultural waste materials. Multiscale Multidisciplinary Model Experiments Des. https://doi.org/10.1007/s41939-023-00327-w
Oyebisi S, Owamah H, Omeje M (2023c) Application of machine learning algorithm in the internal and external hazards from industrial byproducts. Clean Eng Technol 13:100629. https://doi.org/10.1016/j.clet.2023.100629
Panchal G, Ganatra A, Kosta YP, Panchal D (2011) Behaviour Analysis of Multilayer Perceptronswith multiple hidden neurons and hidden layers. Int J Comput Theory Eng 332–337. https://doi.org/10.7763/IJCTE.2011.V3.328
Pavlidou S, Koroneos A, Papastefanou C et al (2006) Natural radioactivity of granites used as building materials. J Environ Radioact 89:48–60. https://doi.org/10.1016/j.jenvrad.2006.03.005
Peppas TK, Karfopoulos KL, Karangelos DJ et al (2010) Radiological and instrumental neutron activation analysis determined characteristics of size-fractionated fly ash. J Hazard Mater 181:255–262. https://doi.org/10.1016/j.jhazmat.2010.05.005
Petropoulos NP, Anagnostakis MJ, Simopoulos SE (2002) Photon attenuation, natural radioactivity content and radon exhalation rate of building materials. J Environ Radioact 61:257–269. https://doi.org/10.1016/S0265-931X(01)00132-1
Puch K-H, Bialucha R, Keller G (2005) Naturally occurring radioactivity in industrial by-products from coal-fired power plants, from municipal waste incineration and from the iron- and steel-industry. 996–1008. https://doi.org/10.1016/S1569-4860(04)07123-2
Puertas F, Alonso MM, Torres-Carrasco M et al (2015) Radiological characterization of anhydrous/hydrated cements and geopolymers. Constr Build Mater 101:1105–1112. https://doi.org/10.1016/j.conbuildmat.2015.10.074
Puertas F, Suárez-Navarro JA, Alonso MM, Gascó C (2021) NORM waste, cements, and concretes. A review. Materiales De Construcción 71:e259. https://doi.org/10.3989/mc.2021.13520
Raheem A, Ikotun B, Oyebisi S, Ede A (2023) Machine learning algorithms in wood ash-cement-Nano TiO2-based mortar subjected to

elevated temperatures. Results Eng 18:101077. https://doi.org/10.1016/j.rineng.2023.101077
Righi S, Bruzzi L (2006) Natural radioactivity and radon exhalation in building materials used in Italian dwellings. J Environ Radioact 88:158–170. https://doi.org/10.1016/j.jenvrad.2006.01.009
Roper AR, Stabin MG, Delapp RC, Kosson DS (2013) Analysis of naturally-occurring Radionuclides in Coal Combustion fly Ash, Gypsum, and Scrubber Residue samples. Health Phys 104:264–269. https://doi.org/10.1097/HP.0b013e318279f3bf
Rubinos DA, Barral MT (2013) Fractionation and mobility of metals in bauxite red mud. Environ Sci Pollut Res 20:7787–7802. https://doi.org/10.1007/s11356-013-1477-4
Sahoo BK, Nathwani D, Eappen KP et al (2007) Estimation of radon emanation factor in Indian building materials. Radiat Meas 42:1422–1425. https://doi.org/10.1016/j.radmeas.2007.04.002
Sanjuán MÁ, Quintana B, Argiz C (2019) Coal bottom ash natural radioactivity in building materials. J Radioanal Nucl Chem 319:91–99. https://doi.org/10.1007/s10967-018-6251-0
Santos AJG, Mazzilli BP, Fávaro DIT, Silva PSC (2006) Partitioning of radionuclides and trace elements in phosphogypsum and its source materials based on sequential extraction methods. J Environ Radioact 87:52–61. https://doi.org/10.1016/j.jenvrad.2005.10.008
Sas Z, Doherty R, Kovacs T et al (2017) Radiological evaluation of by-products used in construction and alternative applications; part I. Preparation of a natural radioactivity database. Constr Build Mater 150:227–237. https://doi.org/10.1016/j.conbuildmat.2017.05.167
Sas Z, Sha W, Soutsos M et al (2019) Radiological characterisation of alkali-activated construction materials containing red mud, fly ash and ground granulated blast-furnace slag. Sci Total Environ 659:1496–1504. https://doi.org/10.1016/j.scitotenv.2019.01.006
Schroeyers W, Sas Z, Bator G et al (2018) The NORM4Building database, a tool for radiological assessment when using by-products in building materials. Constr Build Mater 159:755–767. https://doi.org/10.1016/j.conbuildmat.2017.11.037
Shafi I, Ahmad J, Shah SI, Kashif FM (2006) Impact of varying neurons and hidden layers in neural network architecture for a time frequency application. In: 2006 IEEE International Multitopic Conference. IEEE 188–193. https://doi.org/10.1109/INMIC.2006.358160
Shoeib MY, Thabayneh KM (2014) Assessment of natural radiation exposure and radon exhalation rate in various samples of Egyptian building materials. J Radiat Res Appl Sci 7:174–181. https://doi.org/10.1016/j.jrras.2014.01.004
Singovszka E, Estokova A, Mitterpach J (2017) Radioactivity of buildings materials available in Slovakia. IOP Conf Ser Earth Environ Sci 92:012054. https://doi.org/10.1088/1755-1315/92/1/012054
Sofilić T, Barišić D, Sofilić U (2010) Monitoring of 137Cs in electric arc furnace steel making process. J Radioanal Nucl Chem 284:615–622. https://doi.org/10.1007/s10967-010-0513-9
Solak S, Turhan Ş, Uğur FA et al (2014) Evaluation of potential exposure risks of natural radioactivity levels emitted from building materials used in Adana, Turkey. Indoor Built Environ 23:594–602. https://doi.org/10.1177/1420326X12448075
Somlai J, Jobbágy V, Kovács J et al (2008) Radiological aspects of the usability of red mud as building material additive. J Hazard Mater 150:541–545. https://doi.org/10.1016/j.jhazmat.2007.05.004
Temuujin J, Minjigmaa A, Davaabal B et al (2014) Utilization of radioactive high-calcium Mongolian flyash for the preparation of alkali-activated geopolymers for safe use as construction materials. Ceram Int 40:16475–16483. https://doi.org/10.1016/j.ceramint.2014.07.157
Todorović N, Hansman J, Mrđa D et al (2017) Concentrations of 226 Ra, 232 th and 4 0 K in industrial kaolinized granite. J Environ Radioact 168:10–14. https://doi.org/10.1016/j.jenvrad.2016.07.032
Trevisi R, Risica S, D'Alessandro M et al (2012) Natural radioactivity in building materials in the European Union: a database and an estimate of radiological significance. J Environ Radioact 105:11–20. https://doi.org/10.1016/j.jenvrad.2011.10.001
Trevisi R, Leonardi F, Risica S, Nuccetelli C (2018) Updated database on natural radioactivity in building materials in Europe. J Environ Radioact 187:90–105. https://doi.org/10.1016/j.jenvrad.2018.01.024
Tso MW, Leung JKC (1996) Radiological impact of coal ash from the power plants in Hong Kong. J Environ Radioact 30:1–14. https://doi.org/10.1016/0265-931X(95)00042-9
Tuo F, Peng X, Zhou Q, Zhang J, ASSESSMENT OF NATURAL RADIOACTIVITY LEVELS AND RADIOLOGICAL HAZARDS IN BUILDING MATERIALS (2020) Radiat Prot Dosimetry 188:316–321. https://doi.org/10.1093/rpd/ncz289
Turhan Ş (2008) Assessment of the natural radioactivity and radiological hazards in Turkish cement and its raw materials. J Environ Radioact 99:404–414. https://doi.org/10.1016/j.jenvrad.2007.11.001
Turhan Ş (2009) Radiological impacts of the usability of clay and kaolin as raw material in manufacturing of structural building materials in Turkey. J Radiol Prot 29:75–83. https://doi.org/10.1088/0952-4746/29/1/005
United Nations Scientific Committee on the Effects of Atomic Radiation (2000) Sources and effects of ionizing radiation, United Nations Scientific Committee on the Effects of Atomic Radiation UNSCEAR 2000 Report to the General Assembly, with Scientific Annexes. New York, NY
United Nations Scientific Committee on the Effects of Atomic Radiation (2008) Effects of Ionizing Radiation: Report to the General Assembly, with Scientific Annexes,. New York, NY
United Nations Scientific Committee on the Effects of Atomic Radiation (1993) Sources and Effects of Ionizing Radiation, United Nations Scientific Committee on the Effects of Atomic Radiation UNSCEAR 2000 Report to the General Assembly, with Scientific Annexes. New York, NY
United States Environmental Protection Agency (2008) United States Environmental Protection Agency. Washington, D.C., United States
Uzair M, Jamil N (2020) Effects of Hidden Layers on the Efficiency of Neural networks. In: 2020 IEEE 23rd International Multitopic Conference (INMIC). IEEE 1–6. https://doi.org/10.1109/INMIC50486.2020.9318195
Willmott C, Matsuura K (2005) Advantages of the mean absolute error (MAE) over the root mean square error (RMSE) in assessing average model performance. Clim Res 30:79–82
Xhixha G, Bezzon GP, Broggini C et al (2013) The worldwide NORM production and a fully automated gamma-ray spectrometer for their characterization. J Radioanal Nucl Chem 295:445–457. https://doi.org/10.1007/s10967-012-1791-1
Xinwei L (2004) Natural radioactivity in some building materials and by-products of Shaanxi, China. J Radioanal Nucl Chem 262:775–777. https://doi.org/10.1007/s10967-004-0509-4
Xinwei L, Xiaolan Z (2006) Measurement of natural radioactivity in sand samples collected from the Baoji Weihe Sands Park, China. Environ Geol 50:977–982. https://doi.org/10.1007/s00254-006-0266-5
Yu Q (1996) Investigation on the radioactivity concentration of coal and ash from Shanghai coal-fired power plant, China. J Radiol Med Prot 16:374–375
Zak A, Isajenko K, Piotrowska B et al (2008) Natural radioactivity of wastes. Nukleonika 55:387–391
Zeller B (1995) Radioaktivitätsbilanzen in Steinkohlekraftwerken. Diplomarbeit im FB Technisches Gesundheitswesen, FIZ Gießen-Friedberg